JOURNAL OF GUIDANCE, CONTROL, AND DYNAMICS
Vol. 32, No. 2, March–April 2009

Derivation of the Dynamics Equations of Receiver Aircraft in Aerial Refueling

Jayme Waishek* and Atilla Dogan†
University of Texas at Arlington, Arlington, Texas 76019
and
William Blake‡
U.S. Air Force Research Laboratory, Wright–Patterson Air Force Base, Ohio 45433

DOI: 10.2514/1.35892

A set of equations of motion is derived for an aircraft undergoing aerial refueling. The equations include the time-varying mass and inertia associated with fuel transfer as well as the vortex-induced wind effect from the tanker. They are derived in terms of the translational and rotational position and velocity of the receiver with respect to the tanker. The equations of motion are implemented in an integrated simulation environment with a feedback controller for receiver station keeping as well as a feedback controller to fly the tanker on a U-turn maneuver.

Nomenclature

$\mathcal{E}_R$	=	3×3 matrix, which depends on (V_R, β_R, α_R), see Eq. (37)
$\underline{F}$	=	total external force acting on receiver aircraft
$\underline{H}$	=	angular momentum
$\mathbf{I}_M$	=	inertia matrix of the receiver, excluding fuel, see Eq. (57)
$\mathbf{I}_t$	=	inertia matrix of the receiver including fuel in fuel tanks, see Eq. (58)
$I_{3\times3}$	=	3×3 identity matrix
M	=	mass of solid part of receiver
$\underline{M}$	=	total external moment acting on receiver aircraft
M_i	=	mass of ith particle of the solid part of the receiver
m	=	total mass of fuel
m_j	=	mass of fuel in jth fuel tank
m_{jl}	=	mass of fuel clusters in or entering jth fuel pipe
P	=	origin of B_R frame
$\underline{P}$	=	linear momentum
$\mathbf{R}_{(.)(*)}$	=	rotation matrix from frame $(*)$ to frame $(\cdot)$
$\underline{r}$	=	position relative to the inertial frame
t	=	time
$\underline{U}$	=	velocity of receiver relative to air
V_R	=	airspeed of receiver aircraft
$\underline{V}_{\dot{m}}$	=	velocity of fuel relative to tanker
$\underline{V}_0$	=	inertial velocity of fuel entering receiver aircraft
$\underline{W}$	=	wind velocity
α_R	=	angle of attack of receiver aircraft
β_R	=	side-slip angle of receiver aircraft
Δm_{jl}	=	mass of fuel particles in transition
$\Delta(\cdot)$	=	variation of $(\cdot)$ in Δt time
$\underline{\xi}$	=	position of B_R-frame origin relative to B_T-frame origin
$\underline{\rho}$	=	position relative to origin of B_R frame or B_T frame
τ	=	time constant of reaction time delay model
$\mathcal{X}_R$	=	$[V_R \quad \beta_R \quad \alpha_R]^T$
$\underline{\omega}$	=	angular velocity

Subscripts

B_R	=	body frame of receiver aircraft
B_T	=	body frame of tanker aircraft
B_RB_T	=	body frame of receiver relative to tanker
C	=	fuel port (receptacle) relative to B_T frame
I	=	inertial frame
R	=	fuel port (receptacle) relative to B_R frame
W_R	=	wind frame of receiver aircraft
0	=	origin of inertial frame

Conventions

a	=	representation of vector $\underline{a}$ in a frame in which originally defined, 3×1 array
$\underline{a}$	=	underline indicates vector quantity
$[\underline{a}]_X$	=	time derivative of $\underline{a}$ with respect to X frame
$\mathbf{S}(a)$	=	skew-symmetric matrix constructed with representation a, see Eq. (A3)
$[\hat{\underline{X}}]$	=	vectrix of X frame, $X = \{B_R, B_T, B_RB_T, W_R, I\}$, 3×1 array, see Eq. (21)

Presented as Paper 251 at the 45th AIAA Aerospace Sciences Meeting and Exhibit, Reno, Nevada, 8–11 January 2007; received 27 November 2007; revision received 23 August 2008; accepted for publication 27 August 2008.

*Graduate Student, Department of Mechanical and Aerospace Engineering. Student Member AIAA.
†Assistant Professor, Department of Mechanical and Aerospace Engineering. Senior Member AIAA.
‡Aerospace Engineer. Associate Fellow AIAA.

I. Introduction

AERIAL refueling has been used to extend the range of military aircraft for over 50 years. There is now interest in the research community [1] to develop efficient and robust control algorithms that will enable automated aerial refueling. To develop such algorithms, accurate dynamic models of the tanker and receiver aircraft, as well as the tanker vortex-induced effects, are required. Previous aerial refueling studies [1–4] have investigated tanker–receiver interference, stability of the receiver aircraft, and design of an autonomous refueling controller. To generate useful results from a simulation, it is critical to model the receiver aircraft taking into account all major factors that influence its dynamics. The present work derives equations of motion for the receiver to model 1) the relative motion of the receiver with respect to the tanker, 2) time-varying mass and inertia properties during fuel transfer, and 3) exposure to nonuniform wind induced by the tanker's wake vortices.

Previous formation flight studies [5] have used various methods for studying relative motion. The problem of relative motion is relevant to other applications such as spacecraft formation [6–8] and shipboard landing [9]. A common approach with the cited work is to quantify relative motion through kinematic relations after the

equations of motion are derived for each vehicle separately. In this work, the equations of motion are derived in terms of relative position and orientation.

Mass properties of a system vary when mass transfers into or out of the system or the mass distribution within the system changes. Variable mass systems have been studied extensively in the area of space flight [10–14] and other applications, which show the significance of the mass transfer effect on vehicle dynamics. In the case of aerial refueling, fuel transferred to the receiver aircraft brings in momentum and changes its inertia properties. Earlier aerial refueling studies [1,15,16] either ignore the effect of mass transfer or treat it as disturbance causing parametric uncertainty [1]. In the present work, the equations of motion for the receiver are derived considering the system of the receiver aircraft and the fuel before and after being transferred into the receiver, yielding a generic mathematical model that includes the dynamic effect of fuel transfer.

The dynamic effect of nonuniform wind is also considered in this work. In aerial refueling, the receiver is subject to the nonuniform wind induced by the wake vortex system of the tanker, which can be detrimental to the control of the receiver aircraft [16]. To model the dynamic effect of nonuniform wind, various techniques such as strip theory, averaging, and tables lookup have been used [17–19]. In this work, wind terms appear explicitly in the equations of motion. This enables the implementation of a novel vortex effect modeling technique [20] in the aerial refueling problem. With this technique, the modeling of a nonuniform wind effect is more direct and computationally efficient, and the restrictions on the relative position, orientation, or sizes of the aircraft are removed.

This paper is organized as follows. Equations for translational motion are derived in Sec. II. Section III presents the derivation of the equations for rotational motion. In Sec. IV, the vector equations of motion are converted into matrix form. Section V introduces the paper by Dogan et al. [20], which describes the procedure for approximating the nonuniform wind field induced by wake vortices as a uniform wind field. Section VI explains how the physical design parameters of the receiver aircraft and its fuel tanks are incorporated into the equations of motion and presents simulation results. Finally, Sec. VII presents conclusions based on the simulation results and proposes additional application of the concepts herein addressed.

II. Translational Motion

In aerial refueling, the position of the receiver needs to be controlled relative to the tanker, not relative to the ground. This means the translational kinematics should be written in terms of the position vector of the receiver with respect to the tanker.

Figure 1 depicts the spatial relation of three reference frames: 1) inertial, 2) tanker's body (B_T frame), and 3) receiver's body (B_R frame). The vectorial relation of the origins of the reference frames yields

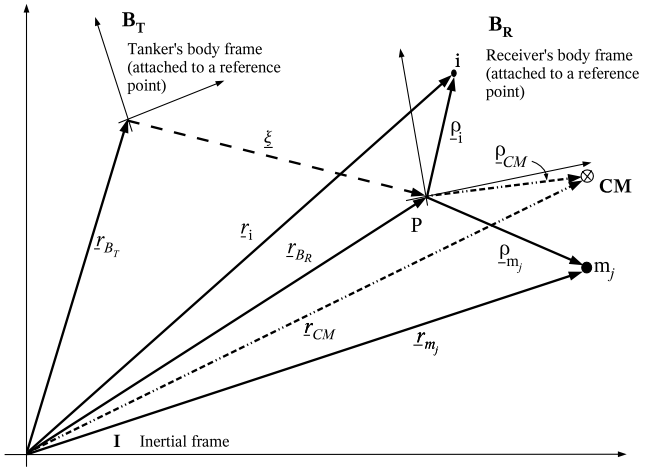

Fig. 1 Intermediate reference frames: tanker and receiver's body frame.

$$\underline{r}_{B_R} = \underline{r}_{B_T} + \underline{\xi} \tag{1}$$

The effect of the wind is incorporated into the kinematics as

$$\dot{\underline{r}}_{B_R} = \underline{U} + \underline{W} \tag{2}$$

The time derivative of Eq. (1) along with Eq. (2) yields

$$\dot{\underline{\xi}} = \underline{U} + \underline{W} - \dot{\underline{r}}_{B_T} \tag{3}$$

which is the translational kinematic equation in terms of the position of the receiver relative to the tanker.

The next step is to derive the translational dynamic equations. The derivation is intended to yield equations with explicit terms to represent the dynamics effect of fuel transfer and wind exposure. Because of fuel transfer in refueling, the receiver aircraft is a system of varying mass. Thus, Newton's second law, which states that force is equal to the time rate of change of momentum, is not directly applicable. However, it can be applied to a system of varying mass by examining the same mass for the change in momentum at two instants of time [13]. This approach is used in this paper by defining a system of constant mass consisting of the receiver aircraft and the fuel added to the receiver through a refueling receptacle in a given time interval. The momenta of this system at time instants $t - \Delta t$ and t, before and after a cluster of fuel particles are added to the receiver, are used to determine the time rate of change of momentum while refueling. The B_R frame is defined to be geometrically fixed in the receiver aircraft and is therefore not necessarily at its c.m. This is to accommodate the fact that the c.m. will be moving during fuel transfer.

To facilitate the derivation of the dynamics equations including the effect of fuel transfer, the receiver aircraft–fuel system is considered, at time $t - \Delta t$, to comprise four parts (see Fig. 2) as 1) solid, 2) fuel about to enter aircraft, 3) fuel in transition, and 4) fuel in fuel tanks. The solid part is considered rigid and represented by n particles with constant masses, M_i $(i = 1, \ldots, n)$, at fixed positions in the B_R frame denoted by $\underline{\rho}_i$. The origin of the B_R frame is chosen to be at the c.m. of the solid part of the receiver aircraft before the fuel transfer starts. Considering that the receiver has k fuel tanks, the fuel about to enter the aircraft is represented by a cluster of k particles with mass Δm_{j0} $(j = 1, \ldots, k)$ entering the aircraft through the receptacle or fuel port at $\underline{\rho}_R$, which is also fixed in the B_R frame. The fuel in transition is represented, for each fuel tank, by a train of h_j particles with mass $m_{jl} + \Delta m_{jl}$ $(l = 1, \ldots, h_j$, where $j = 1, \ldots, k)$ at $\underline{\rho}_{m_{jl}}$ moving through fuel pipes extending from the receptacle to the jth fuel tank. Mass Δm_{jl} represents the amount of fuel that will leave m_{jl} and join $m_{j(l+1)}$ as fuel flows through each pipe. The fuel in fuel tanks is represented by k lumped masses concentrated at the c.m. of fuel in each fuel tank at a given time. Thus, the mass of fuel in the jth fuel tank, m_j $(j = 1, \ldots, k)$, and its position relative to the B_R frame, $\underline{\rho}_{m_j}$, are time varying during refueling.

The linear momentum of the system at time $t - \Delta t$ is

$$\underline{P}_1 = \sum_{i=1}^{n} M_i \dot{\underline{r}}_i + \sum_{j=1}^{k} \left[m_j \dot{\underline{r}}_{m_j} + \sum_{l=1}^{h_j} (m_{jl} + \Delta m_{jl}) \dot{\underline{r}}_{m_{jl}} + \Delta m_{j0} \underline{V}_0 \right] \tag{4}$$

Now, consider the receiver-fuel system depicted in Fig. 2, in the time interval $t - \Delta t$ to t. During this time, the cluster of k fuel particles entering the receiver through the receptacle at $\underline{\rho}_R$ splits into the k particles each with mass Δm_{j0} and each particle joins the jth train in the receptacle side. This means that Δm_{j0} joins m_{j1}. Concurrently, Δm_{j1} leaves m_{j1} and joins m_{j2}, with the other $\Delta m_{j(l-1)}$ particles similarly cascading down the train toward the jth fuel tank. The last particle Δm_{jh_j}, in the fuel tank side of each train, at time $t - \Delta t$ joins m_j in the corresponding fuel tank at time t. Thus, at time t, the linear momentum of the system is

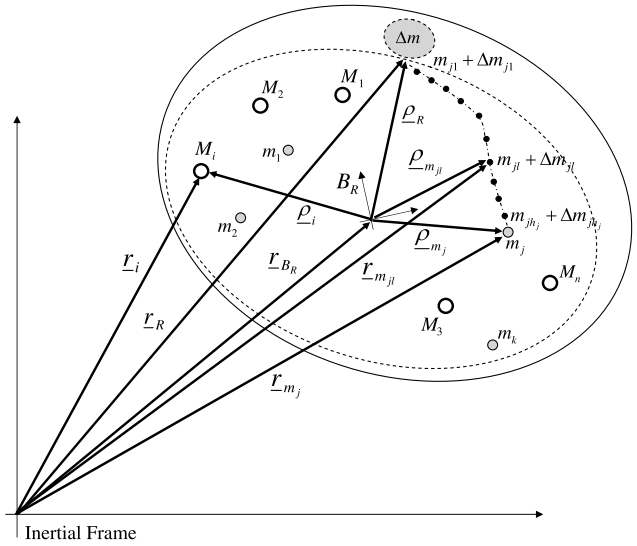

Fig. 2 Receiver-fuel system of constant mass.

$$\underline{P}_2 = \sum_{i=1}^{n} M_i(\underline{\dot{r}}_i + \Delta\underline{\dot{r}}_i) + \sum_{j=1}^{k}\Bigg[(m_j + \Delta m_{jh_j})(\underline{\dot{r}}_{m_j} + \Delta\underline{\dot{r}}_{m_j}) + \sum_{l=1}^{h_j}(m_{jl} + \Delta m_{j(l-1)})(\underline{\dot{r}}_{m_{jl}} + \Delta\underline{\dot{r}}_{m_{jl}})\Bigg] \tag{5}$$

The limit of $\underline{P}_2 - \underline{P}_1$ as Δt goes to zero yields the time rate of change of momentum of the system at time t as

$$\underline{\dot{P}} = \sum_{i=1}^{n} M_i\underline{\ddot{r}}_i + \sum_{j=1}^{k}\Bigg\{\dot{m}_{jh_j}\underline{\dot{r}}_{m_j} + m_j\underline{\ddot{r}}_{m_j} + \sum_{l=1}^{h_j}[(\dot{m}_{j(l-1)} - \dot{m}_{jl})\underline{\dot{r}}_{m_{jl}} + m_{jl}\underline{\ddot{r}}_{m_{jl}}] - \dot{m}_{j0}\underline{V}_0\Bigg\} \tag{6}$$

The fourth and fifth terms on the right-hand side of this equation (summation over l) require the specification of fuel flow through the pipelines, which is not practical in the case of this work. However, the following assumptions reduce the equation to a form that can be easily implemented in dynamic simulation. With the assumption of steady fuel flow, that is, $\dot{m}_{j(l-1)} = \dot{m}_{jl} = \dot{m}_j$ for all $l = 1, \ldots, h_j$, the fourth term becomes zero. This implies that m_{jl} are time invariant as the same amount of mass joins and leaves the clusters simultaneously. Further, in any practical aerial refueling case, the total amount of mass that occupies the fuel pipes should be very small relative the sum of the masses of the empty aircraft and the fuel in the fuel tanks. Thus, $m_{jl}\underline{\ddot{r}}_{m_{jl}}$ terms can be ignored. In such a case, Eq. (6), which is the translational dynamics equation of the receiver aircraft, becomes

$$\underline{F} = M\underline{\ddot{r}}_{B_R} + \sum_{j=1}^{k}(\dot{m}_j\underline{\dot{r}}_{m_j} + m_j\underline{\ddot{r}}_{m_j}) - \dot{m}\underline{V}_0 \tag{7}$$

where

$$\dot{m} = \sum_{j=1}^{k}\dot{m}_{j0}$$

is the total fuel flow rate into the receiver.

There are three drawbacks with the translational dynamics equation as presented in Eq. (7). First, masses m_j ($j = 1, \ldots, k$) will be used to represent the fuel transferred into the fuel tanks, which are located in the receiver aircraft. This implies that the velocity and acceleration of the m_j masses will be easier to formulate in the B_R frame than in the inertial frame. Thus, $\underline{r}_{m_j}$ in the second and third terms should be written in terms of the position vectors with respect to the B_R frame. From Fig. 2, it is seen that

$$\underline{r}_{m_j} = \underline{r}_{B_R} + \underline{\rho}_{m_j} \tag{8}$$

Second, it is easier to express the fuel flow velocity in the tanker frame; hence,

$$\underline{V}_0 = \underline{\dot{r}}_{B_T} + \underline{V}_{\dot{m}} + \underline{\omega}_{B_T} \times \underline{\rho}_C \tag{9}$$

where $\underline{\rho}_C$ is measured from the origin of the tanker's body frame. Substituting Eqs. (8) and (9) into Eq. (7) and rearranging yields

$$(M + m)\underline{\ddot{r}}_{B_R} = \underline{F} - \dot{m}(\underline{\dot{r}}_{B_R} - \underline{\dot{r}}_{B_T} - \underline{V}_{\dot{m}} - \underline{\omega}_{B_T} \times \underline{\rho}_C) - \sum_{j=1}^{k}(\dot{m}_j\underline{\dot{\rho}}_{m_j} + m_j\underline{\ddot{\rho}}_{m_j}) \tag{10}$$

As a special case, $\dot{m} = \dot{m}_j = 0$ when the fuel transfer is completed. Then, Eq. (10) becomes

$$(M + m)\underline{\ddot{r}}_{B_R} = \underline{F} - \sum_{j=1}^{k} m_j\underline{\ddot{\rho}}_{m_j} \tag{11}$$

where the second term is due to the fact that the c.m. of the receiver is no longer at point P. Further, when the fuel tanks are positioned in such a way that the c.m. of the fuel is at point P,

$$\sum_{j=1}^{k} m_j\underline{\rho}_{m_j} = 0$$

which implies that

$$\sum_{j=1}^{k} m_j\underline{\ddot{\rho}}_{m_j} = 0$$

since m_j ($j = 1, \ldots, k$) are constant in this special case. Thus, the translational dynamics as represented in Eq. (10) is reduced to

$$(M + m)\underline{\ddot{r}}_{B_R} = \underline{F} \tag{12}$$

as expected.

Third, the effect of the wind can be factored into the analysis by writing $\underline{\dot{r}}_{B_R}$ and $\underline{\ddot{r}}_{B_R}$ in terms of the airspeed of the receiver and the wind acting on it. To do this, Eq. (2) is differentiated to get

$$\underline{\ddot{r}}_{B_R} = \underline{\dot{U}} + \underline{\dot{W}} \tag{13}$$

Equations (2) and (13) are substituted into Eq. (10) and the result is rearranged to have $\underline{\dot{U}}$ on the left-hand side. This results in the general translational dynamics equation:

$$\underline{\dot{U}} = \frac{1}{(M + m)}\Bigg[\underline{F} - \dot{m}(\underline{U} + \underline{W} - \underline{\dot{r}}_{B_T} - \underline{V}_{\dot{m}} - \underline{\omega}_{B_T} \times \underline{\rho}_C) - \sum_{j=1}^{k}(\dot{m}_j\underline{\dot{\rho}}_{m_j} + m_j\underline{\ddot{\rho}}_{m_j})\Bigg] - \underline{\dot{W}} \tag{14}$$

The resultant force $\underline{F}$ in Eq. (14) is considered to be the sum of the gravity force vector, the aerodynamic force vector, and the propulsive force vector.

Several remarks can be made regarding Eq. (14). First, the terms containing $\dot{m}_j$ and $\dot{m}$ represent the effect of fuel transfer on the translational dynamics of the receiver aircraft. For the aerial refueling scenario, as an example, $\dot{m}_j$, the rate of mass change can be approximated as equal to the fuel transfer rate into the jth fuel tank. This modular formulation facilitates the simulation of asymmetric fuel loading conditions. In practice, the values of $\dot{m}_j$, $\underline{\rho}_{m_j}$, $\underline{\dot{\rho}}_{m_j}$, and $\underline{\ddot{\rho}}_{m_j}$ depend on the shape, size, and location of the fuel tanks on the

receiver aircraft and also the individual rates of fuel flow into each fuel tank on the receiver.

III. Rotational Motion

For the derivation of the equations of rotational dynamics, the definitions of the receiver-fuel system and the reference frames, introduced for translational dynamics, are used. It can then be stated that the external moment is equal to the time rate of change of the angular momentum because the angular momentum of a definite mass is examined for its rate of change [13].

In a manner which parallels the translational dynamics derivation, the angular momenta of the system right before and after fuel joins the receiver are used to determine the time rate of change of the angular momentum. At time $t - \Delta t$, the angular momentum of the system around the origin of the inertial frame is

$$\underline{H}_1 = \sum_{i=1}^{n} \underline{r}_i \times M_i \underline{\dot{r}}_i + \underline{r}_R \times \sum_{j=1}^{k} \Delta m_{j0} \underline{V}_0 + \sum_{j=1}^{k} \sum_{l=1}^{h_j} \underline{r}_{m_{jl}} \times \Delta m_{jl} \underline{\dot{r}}_{m_{jl}} + \sum_{j=1}^{k} \underline{r}_{m_j} \times m_j \underline{\dot{r}}_{m_j} \tag{15}$$

where each term represents the moment of the corresponding linear momentum term in Eq. (4) about the origin of the inertial frame. At time t, the angular momentum of the system is

$$\underline{H}_2 = \sum_{i=1}^{n} (\underline{r}_i + \Delta \underline{r}_i) \times M_i (\underline{\dot{r}}_i + \Delta \underline{\dot{r}}_i) + \sum_{j=1}^{k} \sum_{l=1}^{h_j} (\underline{r}_{m_{jl}} + \Delta \underline{r}_{m_{jl}}) \times \Delta m_{j(l-1)} (\underline{\dot{r}}_{m_{jl}} + \Delta \underline{\dot{r}}_{m_{jl}}) + \sum_{j=1}^{k} (\underline{r}_{m_j} + \Delta \underline{r}_{m_j}) \times (m_j + \Delta m_{jh_j}) (\underline{\dot{r}}_{m_j} + \Delta \underline{\dot{r}}_{m_j}) \tag{16}$$

The limit of the difference in angular momenta at $t - \Delta t$ and t as Δt goes to zero results in the time rate of change of momentum of the system at time t, which is equal to the moment acting on the system at the same time. Under the same assumptions stated for the translational dynamics, the rotational dynamics equation becomes

$$\underline{M}_0 = \sum_{i=1}^{n} \underline{r}_i \times M_i \underline{\ddot{r}}_i + \sum_{j=1}^{k} \underline{r}_{m_j} \times \dot{m}_j \underline{\dot{r}}_{m_j} + \sum_{j=1}^{k} \underline{r}_{m_j} \times m_j \underline{\ddot{r}}_{m_j} - \underline{r}_R \times \dot{m} \underline{V}_0 \tag{17}$$

Note that

$$\underline{M}_{B_R} = \underline{M}_0 - \underline{r}_{B_R} \times \underline{F} \tag{18}$$

Substituting $\underline{M}_0$ from Eq. (17) and $\underline{F}$ from Eq. (7) into Eq. (18) and using the expression for $\underline{V}_0$ from Eq. (9) yields

$$\underline{M}_{B_R} = \sum_{i=1}^{n} \underline{\rho}_i \times M_i (\underline{\ddot{r}}_{B_R} + \underline{\ddot{\rho}}_i) + \sum_{j=1}^{k} \underline{\rho}_{m_j} \times [\dot{m}_j (\underline{\dot{r}}_{B_R} + \underline{\dot{\rho}}_{m_j}) + m_j (\underline{\ddot{r}}_{B_R} + \underline{\ddot{\rho}}_{m_j})] - \underline{\rho}_R \times \dot{m} (\underline{\dot{r}}_{B_T} + \underline{V}_{\dot{m}} + \underline{\omega}_{B_T} \times \underline{\rho}_C) \tag{19}$$

Further, substituting $\underline{\dot{r}}_{B_R}$ and $\underline{\ddot{r}}_{B_R}$ from Eqs. (2) and (13), respectively, into Eq. (19) yields the rotational dynamics with explicit wind terms as

$$\underline{M}_{B_R} = \sum_{i=1}^{n} \underline{\rho}_i \times M_i (\underline{\dot{U}} + \underline{\dot{W}} + \underline{\ddot{\rho}}_i) + \sum_{j=1}^{k} \underline{\rho}_{m_j} \times [\dot{m}_j (\underline{U} + \underline{W} + \underline{\dot{\rho}}_{m_j}) + m_j (\underline{\dot{U}} + \underline{\dot{W}} + \underline{\ddot{\rho}}_{m_j})] - \underline{\rho}_R \times \dot{m} (\underline{\dot{r}}_{B_T} + \underline{V}_{\dot{m}} + \underline{\omega}_{B_T} \times \underline{\rho}_C) \tag{20}$$

In the special case when $\dot{m} = \dot{m}_j = 0$, both types of masses at n points and k points have the same effect in the rotational dynamics and the equation becomes the rotational dynamics of a system of $n + k$ concentrated masses.

The total moment of the external forces about the origin of the B_R frame can be written as the vectorial sum of the moment vectors due to gravity, aerodynamics, and propulsion. The moment due to gravity is not zero because the origin of the B_R frame is not necessarily at the c.m. of the receiver. However, the c.m. of the rigid body particles is, by definition, the origin of the B_R frame. Therefore, the gravitational moment is only due to the masses concentrated at the k points.

IV. Equations of Motion in Matrix Form

In the preceding sections, the translational and rotational equations of motion are derived in vector form. In this section, these equations are converted into matrix form because matrix equations are more suitable for implementation in simulation software such as MATLAB/Simulink.

To write vector equations in matrix form, vectrix formalism is employed. The vectrix of the X frame is defined to be the array of the unit vectors of its axes and is denoted by

$$[\underline{\hat{X}}] = \begin{bmatrix} \hat{\imath}_X \\ \hat{\jmath}_X \\ \hat{k}_X \end{bmatrix} \tag{21}$$

Hence, vector $\underline{a}$ can be written as

$$\underline{a} = [\underline{\hat{X}}]^T a \tag{22}$$

The relationship between the vectrices of any two frames is defined by the rotation matrix between the two frames, namely,

$$[\underline{\hat{X}}] = \mathbf{R}_{\mathbf{XY}} [\underline{\hat{Y}}] \tag{23}$$

The same holds for representations of a vector in the same two frames.

A. Translational Kinematics

The motion of the receiver relative to the tanker can be expressed easily in the B_T frame; hence, vector $\underline{\xi}$ is expressed in the B_T frame, namely, $\underline{\xi} = [\underline{\hat{B}}_T]^T \xi$. The time derivative of $\underline{\xi}$ in Eq. (3) is with respect to the inertial frame. Thus,

$$\underline{\dot{\xi}} = [\underline{\dot{\xi}}]_{B_T} + \underline{\omega}_{B_T} \times \underline{\xi} \tag{24}$$

or, using the expression of the vector product introduced in Eq. (A2) in Appendix A,

$$\underline{\dot{\xi}} = [\underline{\hat{B}}_T]^T \dot{\xi} - [\underline{\hat{B}}_T]^T \mathbf{S}(\omega_{B_T}) \xi \tag{25}$$

For the three velocity vectors on the right-hand side of Eq. (3), three different frames are used to define the representations. The representation of $\underline{U}$ in the W_R frame is used, that is, $\underline{U} = [\underline{\hat{W}}_R]^T U$. The wind vector $\underline{W}$ is expressed in the B_R frame as $\underline{W} = [\underline{\hat{B}}_R]^T W$. The velocity vector of the tanker $\underline{\dot{r}}_{B_T}$ is expressed in the inertial frame as $\underline{\dot{r}}_{B_T} = [\underline{\hat{I}}]^T \dot{r}_{B_T}$. Then, substituting $\underline{\dot{\xi}}$ from Eq. (25), Eq. (3) is rewritten as

$$[\underline{\hat{B}}_T]^T [\dot{\xi} - \mathbf{S}(\omega_{B_T}) \xi] = [\underline{\hat{W}}_R]^T U + [\underline{\hat{B}}_R]^T W - [\underline{\hat{I}}]^T \dot{r}_{B_T} \tag{26}$$

Next, all the terms are written in terms of the same vectrix. Note that $[\underline{\hat{B}}_R] = \mathbf{R}_{\mathbf{B_R B_T}} [\underline{\hat{B}}_T]$, $[\underline{\hat{B}}_T] = \mathbf{R}^{\mathbf{T}}_{\mathbf{B_R B_T}} \mathbf{R}_{\mathbf{B_R W_R}} [\underline{\hat{W}}_R]$, and $[\underline{\hat{B}}_T] = \mathbf{R}_{\mathbf{B_T I}} [\underline{\hat{I}}]$. Equation (26) now becomes

$$[\underline{\hat{B}}_T]^T [\dot{\xi} - \mathbf{S}(\omega_{B_T}) \xi] = [\underline{\hat{B}}_T]^T \mathbf{R}^{\mathbf{T}}_{\mathbf{B_R B_T}} \mathbf{R}_{\mathbf{B_R W_R}} U + [\underline{\hat{B}}_T]^T \mathbf{R}^{\mathbf{T}}_{\mathbf{B_R B_T}} W - [\underline{\hat{B}}_T]^T \mathbf{R}_{\mathbf{B_T I}} \dot{r}_{B_T} \tag{27}$$

which, after canceling the common vectrices, leads to the matrix form of the equations of the translational motion as

$$\dot{\xi} = \mathbf{R}^{\mathbf{T}}_{\mathbf{B_R B_T}} \mathbf{R}_{\mathbf{B_R W_R}} U + \mathbf{R}^{\mathbf{T}}_{\mathbf{B_R B_T}} W - \mathbf{R}_{\mathbf{B_T I}} \dot{r}_{B_T} + \mathbf{S}(\omega_{\mathbf{B_T}})\xi \quad (28)$$

B. Rotational Kinematics

As in the case of translational motion, the rotational motion of the receiver aircraft is formulated relative to the tanker aircraft. Thus, the rotational kinematical differential equations take the form of Poisson's equation

$$\dot{\mathbf{R}}_{\mathbf{B_R B_T}} = \mathbf{S}(\omega_{\mathbf{B_R B_T}})\mathbf{R}_{\mathbf{B_R B_T}} \quad (29)$$

where both the orientation and the angular velocity of the receiver are relative to the tanker.

The angular velocity of the receiver relative to the inertial frame can be expressed as

$$\underline{\omega}_{B_R} = \underline{\omega}_{B_R B_T} + \underline{\omega}_{B_T} \quad (30)$$

The matrix form of this equation is

$$\omega_{B_R} = \omega_{B_R B_T} + \mathbf{R}_{\mathbf{B_R B_T}} \omega_{B_T} \quad (31)$$

where ω_{B_R} and $\omega_{B_R B_T}$ are the representations in the B_R frame and ω_{B_T} is the representation in the B_T frame. From Eqs. (29) and (31), the relations between the angular accelerations are obtained as

$$\dot{\omega}_{B_R} = \dot{\omega}_{B_R B_T} + \mathbf{S}(\omega_{\mathbf{B_R B_T}})\mathbf{R}_{\mathbf{B_R B_T}}\omega_{B_T} + \mathbf{R}_{\mathbf{B_R B_T}}\dot{\omega}_{B_T} \quad (32)$$

C. Translational Dynamics

The translational kinematic equation is written in Eq. (28) in terms of U and $\mathbf{R}_{\mathbf{B_R W_R}}$. Note that U is the representation in the W_R frame. Thus,

$$U = [\, V_R \quad 0 \quad 0 \,]^T \quad (33)$$

This is because the x axis of the W_R frame, by definition, is along the velocity of the receiver relative to the air. Note also that $\mathbf{R}_{\mathbf{B_R W_R}}$ is parameterized by α_R and β_R. In this section, the matrix form of the translational dynamic equation of Eq. (14) is written in terms of $\mathcal{X}_R$. To do this, every vector in Eq. (14) is expressed with $[\hat{I}]^T$ to enable the elimination of the vectrices from the equation. Recall that $\underline{U} = [\underline{\hat{W}_R}]^T U$ and can be expressed as

$$\underline{U} = [\hat{I}]^T \mathbf{R}^{\mathbf{T}}_{\mathbf{B_T I}} \mathbf{R}^{\mathbf{T}}_{\mathbf{B_R B_T}} \mathbf{R}_{\mathbf{B_R W_R}} U \quad (34)$$

Hence,

$$\begin{aligned}\dot{\underline{U}} = [\hat{I}]^T (&\dot{\mathbf{R}}^{\mathbf{T}}_{\mathbf{B_T I}} \mathbf{R}^{\mathbf{T}}_{\mathbf{B_R B_T}} \mathbf{R}_{\mathbf{B_R W_R}} U + \mathbf{R}^{\mathbf{T}}_{\mathbf{B_T I}} \dot{\mathbf{R}}^{\mathbf{T}}_{\mathbf{B_R B_T}} \mathbf{R}_{\mathbf{B_R W_R}} U \\ &+ \mathbf{R}^{\mathbf{T}}_{\mathbf{B_T I}} \mathbf{R}^{\mathbf{T}}_{\mathbf{B_R B_T}} \dot{\mathbf{R}}_{\mathbf{B_R W_R}} U + \mathbf{R}^{\mathbf{T}}_{\mathbf{B_T I}} \mathbf{R}^{\mathbf{T}}_{\mathbf{B_R B_T}} \mathbf{R}_{\mathbf{B_R W_R}} \dot{U})\end{aligned} \quad (35)$$

It can be shown that

$$\dot{\mathbf{R}}_{\mathbf{B_R W_R}} U + \mathbf{R}_{\mathbf{B_R W_R}} \dot{U} = \mathcal{E}_{\mathbf{R}} \dot{\mathcal{X}}_{\mathbf{R}} \quad (36)$$

where

$$\mathcal{E}_{\mathbf{R}} = \begin{bmatrix} \cos\beta_R \cos\alpha_R & -V_R \sin\beta_R \cos\alpha_R & -V_R \cos\beta_R \sin\alpha_R \\ \sin\beta_R & V_R \cos\beta_R & 0 \\ \cos\beta_R \sin\alpha_R & -V_R \sin\beta_R \sin\alpha_R & V_R \cos\beta_R \cos\alpha_R \end{bmatrix} \quad (37)$$

From Poisson's equation for the rotational kinematics of the tanker,

$$\dot{\mathbf{R}}_{\mathbf{B_T I}} = \mathbf{S}(\omega_{\mathbf{B_T}})\mathbf{R}_{\mathbf{B_T I}} \quad (38)$$

Using Eqs. (29), (36), and (38) in Eq. (35) yields

$$\begin{aligned}\dot{\underline{U}} = [\hat{I}]^T \mathbf{R}^{\mathbf{T}}_{\mathbf{B_T I}} \{ &-[\mathbf{R}^{\mathbf{T}}_{\mathbf{B_R B_T}} \mathbf{S}(\omega_{\mathbf{B_R B_T}}) + \mathbf{S}(\omega_{\mathbf{B_T}}) \mathbf{R}^{\mathbf{T}}_{\mathbf{B_R B_T}}] \mathbf{R}_{\mathbf{B_R W_R}} U \\ &+ \mathbf{R}^{\mathbf{T}}_{\mathbf{B_R B_T}} \mathcal{E}_{\mathbf{R}} \dot{\mathcal{X}}_R \}\end{aligned} \quad (39)$$

Next, recalling that $\underline{W} = [\underline{\hat{B}_R}]^T W$, one can write

$$\underline{W} = [\hat{I}]^T \mathbf{R}^{\mathbf{T}}_{\mathbf{B_T I}} \mathbf{R}^{\mathbf{T}}_{\mathbf{B_R B_T}} W \quad (40)$$

Taking the derivative of Eq. (40) and using Eqs. (29) and (38) yields

$$\begin{aligned}\dot{\underline{W}} = [\hat{I}]^T \mathbf{R}^{\mathbf{T}}_{\mathbf{B_T I}} \{ &-[\mathbf{R}^{\mathbf{T}}_{\mathbf{B_R B_T}} \mathbf{S}(\omega_{\mathbf{B_R B_T}}) + \mathbf{S}(\omega_{\mathbf{B_T}}) \mathbf{R}^{\mathbf{T}}_{\mathbf{B_R B_T}}] W \\ &+ \mathbf{R}^{\mathbf{T}}_{\mathbf{B_R B_T}} \dot{W} \}\end{aligned} \quad (41)$$

Two other vectors on the right-hand side of Eq. (14), $\underline{F}$ and $\underline{\dot{r}}_{B_T}$, are expressed in the inertial frame, that is, $\underline{F} = [\hat{I}]^T F$ and $\underline{\dot{r}}_{B_T} = [\hat{I}]^T \dot{r}_{B_T}$. For $\underline{V}_{\dot{m}}$, the most convenient frame is the B_T frame, that is, $\underline{V}_{\dot{m}} = [\underline{\hat{B}_T}]^T V_{\dot{m}}$, which is expressed in the inertial frame as $\underline{V}_{\dot{m}} = [\hat{I}]^T \mathbf{R}^{\mathbf{T}}_{\mathbf{B_T I}} V_{\dot{m}}$. Similarly, $\underline{\omega}_{B_T} \times \underline{\rho}_C = -[\hat{I}]^T \mathbf{R}^{\mathbf{T}}_{\mathbf{B_T I}} \mathbf{S}(\omega_{\mathbf{B_T}}) \rho_C$. The most convenient frame to express the position vector $\underline{\rho}_{m_j}$ is obviously the B_R frame; thus, $\underline{\rho}_{m_j} = [\underline{\hat{B}_R}]^T \rho_{m_j}$. Then, the first and second derivatives of $\underline{\rho}_{m_j}$ can be written as

$$\underline{\dot{\rho}}_{m_j} = [\underline{\dot{\rho}}_{m_j}]_{B_R} + \underline{\omega}_{B_R} \times \underline{\rho}_{m_j} \quad (42)$$

$$\begin{aligned}\underline{\ddot{\rho}}_{m_j} = &[\underline{\ddot{\rho}}_{m_j}]_{B_R} + 2\underline{\omega}_{B_R} \times [\underline{\dot{\rho}}_{m_j}]_{B_R} + \underline{\dot{\omega}}_{B_R} \times \underline{\rho}_{m_j} \\ &+ \underline{\omega}_{B_R} \times (\underline{\omega}_{B_R} \times \underline{\rho}_{m_j})\end{aligned} \quad (43)$$

Substituting $\underline{\omega}_{B_R}$ from Eq. (30), Eq. (42) can be written in vectrix form,

$$\begin{aligned}\underline{\dot{\rho}}_{m_j} = &[\hat{I}]^T \mathbf{R}^{\mathbf{T}}_{\mathbf{B_T I}} \mathbf{R}^{\mathbf{T}}_{\mathbf{B_R B_T}} [\dot{\rho}_{m_j} - \mathbf{S}(\omega_{\mathbf{B_R B_T}})\rho_{m_j} \\ &- \mathbf{R}_{\mathbf{B_R B_T}} \mathbf{S}(\omega_{\mathbf{B_T}}) \mathbf{R}^{\mathbf{T}}_{\mathbf{B_R B_T}} \rho_{m_j}]\end{aligned} \quad (44)$$

Similarly, Eq. (43) can be rewritten as

$$\begin{aligned}\underline{\ddot{\rho}}_{m_j} = &[\hat{I}]^T \mathbf{R}^{\mathbf{T}}_{\mathbf{B_T I}} \{ \mathbf{R}^{\mathbf{T}}_{\mathbf{B_R B_T}} \ddot{\rho}_{m_j} + \mathbf{R}^{\mathbf{T}}_{\mathbf{B_R B_T}} \mathbf{S}(\omega_{\mathbf{B_R B_T}}) [\mathbf{S}(\omega_{\mathbf{B_R B_T}})\rho_{m_j} \\ &- 2\dot{\rho}_{m_j}] + 2\mathbf{S}(\omega_{\mathbf{B_T}}) \mathbf{R}^{\mathbf{T}}_{\mathbf{B_R B_T}} [\mathbf{S}(\omega_{\mathbf{B_R B_T}})\rho_{m_j} - \dot{\rho}_{m_j}] \\ &+ [\mathbf{S}^2(\omega_{\mathbf{B_T}}) - \mathbf{S}(\dot{\omega}_{\mathbf{B_T}})] \mathbf{R}^{\mathbf{T}}_{\mathbf{B_R B_T}} \rho_{m_j} + \mathbf{R}^{\mathbf{T}}_{\mathbf{B_R B_T}} \mathbf{S}(\rho_{m_j}) \dot{\omega}_{B_R B_T} \}\end{aligned} \quad (45)$$

Additionally, the following two properties are used to obtain this equation:

$$\underline{\dot{\omega}}_{B_R B_T} = [\underline{\dot{\omega}}_{B_R B_T}]_{B_R} + \underline{\omega}_{B_T} \times \underline{\omega}_{B_R B_T} \quad (46)$$

$$\begin{aligned}&(\underline{\omega}_{B_T} \times \underline{\omega}_{B_R B_T}) \times \underline{\rho}_{m_j} + \underline{\omega}_{B_R B_T} \times (\underline{\omega}_{B_T} \times \underline{\rho}_{m_j}) \\ &+ \underline{\omega}_{B_T} \times (\underline{\omega}_{B_R B_T} \times \underline{\rho}_{m_j}) = 2\underline{\omega}_{B_T} \times (\underline{\omega}_{B_R B_T} \times \underline{\rho}_{m_j})\end{aligned} \quad (47)$$

Writing all the vectors in vectrix form in Eq. (14), eliminating the common vectrix $[\hat{I}]$, and rearranging, yields the matrix form of the translational dynamic equation

$$\begin{aligned}\dot{\mathcal{X}}_R = &\mathcal{E}^{-1}_{\mathbf{R}} [\mathbf{S}(\omega_{\mathbf{B_R B_T}}) + \mathbf{S}(\mathbf{R}_{\mathbf{B_R B_T}} \omega_{\mathbf{B_T}})](\mathbf{R}_{\mathbf{B_R W_R}} U + W) - \mathcal{E}^{-1}_{\mathbf{R}} \dot{W} \\ &+ \frac{1}{(M+m)} \mathcal{E}^{-1}_{\mathbf{R}} [\mathbf{R}_{\mathbf{B_R B_T}} \mathbf{R}_{\mathbf{B_T I}} (F + \dot{m}\dot{r}_{B_T}) - \dot{m}(\mathbf{R}_{\mathbf{B_R W_R}} U \\ &+ W - \mathbf{R}_{\mathbf{B_R B_T}} V_{\dot{m}} + \mathbf{R}^{\mathbf{T}}_{\mathbf{B_R B_T}} \mathbf{S}(\omega_{\mathbf{B_T}})\rho_C)] \\ &- \frac{1}{(M+m)} \mathcal{E}^{-1}_{\mathbf{R}} \sum_{j=1}^{k} (\dot{m}_j \{\dot{\rho}_{m_j} - [\mathbf{S}(\omega_{\mathbf{B_R B_T}}) + \mathbf{S}(\mathbf{R}_{\mathbf{B_R B_T}} \omega_{\mathbf{B_T}})]\rho_{m_j}\} \\ &+ m_j \{\ddot{\rho}_{m_j} + \mathbf{S}(\omega_{\mathbf{B_R B_T}})[\mathbf{S}(\omega_{\mathbf{B_R B_T}})\rho_{m_j} - 2\dot{\rho}_{m_j}] \\ &+ 2\mathbf{S}(\mathbf{R}_{\mathbf{B_R B_T}} \omega_{\mathbf{B_T}})[\mathbf{S}(\omega_{\mathbf{B_R B_T}})\rho_{m_j} - \dot{\rho}_{m_j}] + [\mathbf{S}^2(\mathbf{R}_{\mathbf{B_R B_T F}} \omega_{\mathbf{B_T}}) \\ &- \mathbf{S}(\mathbf{R}_{\mathbf{B_R B_T}} \dot{\omega}_{\mathbf{B_T}})]\rho_{m_j} + \mathbf{S}(\rho_{\mathbf{m_j}})\dot{\omega}_{B_R B_T}\})\end{aligned} \quad (48)$$

Two additional observations may be made about Eq. (48). First, the explicit dependency of the translational motion of the receiver aircraft on its rotational dynamics states and their time derivatives can be seen through the terms containing $\omega_{B_R B_T}$ and $\dot{\omega}_{B_R B_T}$. Secondly, information about the motion of the tanker aircraft, both translational and rotational, are passed as exogenous inputs to the receiver aircraft. The variables included in this category are $\dot{r}_{B_T}$, $\mathbf{R_{B_T I}}$, ω_{B_T}, and $\dot{\omega}_{B_T}$.

D. Rotational Dynamics

The rotational dynamic equation in Eq. (20) includes the derivatives of $\underline{\rho}_i$ and $\underline{\rho}_{m_j}$. The first and second derivatives of $\underline{\rho}_{m_j}$ are given in Eqs. (42) and (43) in the previous section. Because the $\underline{\rho}_i$ vectors are fixed in the B_R frame, Eqs. (42) and (43) imply that

$$\dot{\underline{\rho}}_i = \underline{\omega}_{B_R} \times \underline{\rho}_i \tag{49}$$

$$\ddot{\underline{\rho}}_i = \dot{\underline{\omega}}_{B_R} \times \underline{\rho}_i + \underline{\omega}_{B_R} \times (\underline{\omega}_{B_R} \times \underline{\rho}_i) \tag{50}$$

Once the derivatives of $\underline{\rho}_{m_j}$ and $\underline{\rho}_i$ are substituted from Eqs. (42), (43), (49), and (50), Eq. (20) becomes

$$\begin{aligned}\underline{M}_{B_R} = &\textstyle\sum_{i=1}^{n}\{\underline{\rho}_i \times M_i[\dot{\underline{U}} + \dot{\underline{W}} + \dot{\underline{\omega}}_{B_R} \times \underline{\rho}_i + \underline{\omega}_{B_R} \times (\underline{\omega}_{B_R} \times \underline{\rho}_i)]\} \\ &+ \sum_{j=1}^{k} \underline{\rho}_{m_j} \times \{\dot{m}_j(\underline{U} + \underline{W} + [\dot{\underline{\rho}}_{m_j}]_{B_R} + \underline{\omega} \times \underline{\rho}_{m_j}) \\ &+ m_j[\dot{\underline{U}} + \dot{\underline{W}} + [\ddot{\underline{\rho}}_{m_j}]_{B_R} + 2\underline{\omega}_{B_R} \times [\dot{\underline{\rho}}_{m_j}]_{B_R} + \dot{\underline{\omega}}_{B_R} \times \underline{\rho}_{m_j} \\ &+ \underline{\omega}_{B_R} \times (\underline{\omega}_{B_R} \times \underline{\rho}_{m_j})]\} - \underline{\rho}_R \times \dot{m}(\dot{\underline{r}}_{B_T} + \underline{V}_{\dot{m}} + \underline{\omega}_{B_T} \times \underline{\rho}_C)\end{aligned} \tag{51}$$

The first line of Eq. (51) can be expanded as

$$\begin{aligned}&\sum_{i=1}^{n}\{\underline{\rho}_i \times M_i(\dot{\underline{U}} + \dot{\underline{W}}) + M_i\underline{\rho}_i \times (\dot{\underline{\omega}}_{B_R} \times \underline{\rho}_i) \\ &\quad + M_i\underline{\rho}_i \times [\underline{\omega}_{B_R} \times (\underline{\omega}_{B_R} \times \underline{\rho}_i)]\}\end{aligned} \tag{52}$$

where the first term is zero because

$$\sum_{i=1}^{n} M_i\underline{\rho}_i = 0$$

The second term can be simplified as

$$\begin{aligned}M_i\underline{\rho}_i \times (\dot{\underline{\omega}}_{B_R} \times \underline{\rho}_i) &= M_i[(\underline{\rho}_i \cdot \underline{\rho}_i)\dot{\underline{\omega}}_{B_R} - (\underline{\rho}_i \cdot \dot{\underline{\omega}}_{B_R})\underline{\rho}_i] \\ &= [\underline{\hat{B}}_R]^T\{M_i[(\rho_i^T\rho_i)\mathbf{I}_{3\times3} - \rho_i\rho_i^T]\dot{\omega}_{B_R}\}\end{aligned} \tag{53}$$

Moreover, the third term in Eq. (52) can be simplified using Eqs. (A1), (A2), and (A5) as

$$M_i\underline{\rho}_i \times [\underline{\omega}_{B_R} \times (\underline{\omega}_{B_R} \times \underline{\rho}_i)] = [\underline{\hat{B}}_R]^T\mathbf{S}(\omega_{\mathbf{B_R}})M_i(\rho_i\rho_i^T)\omega_{B_R} \tag{54}$$

By adding and subtracting $(\rho_i^T\rho_i)\omega_{B_R}$ to the right-hand side of Eq. (54) and rearranging, one obtains

$$-[\underline{\hat{B}}_R]^T\mathbf{S}(\omega_{\mathbf{B_R}})\{M_i[(\rho_i^T\rho_i)\mathbf{I}_{3\times3} - \rho_i\rho_i^T]\omega_{B_R} - M_i(\rho_i^T\rho_i)\omega_{B_R}\} \tag{55}$$

The second term of Eq. (55) is zero because $M_i(\rho_i^T\rho_i)$ is a scalar quantity and $\mathbf{S}(\omega_{\mathbf{B_R}})\omega_{B_R}$ is zero. By substituting Eqs. (53) and (55) into Eq. (52), the first line can be rewritten as

$$\begin{aligned}[\underline{\hat{B}}_R]^T\Bigg\{&\sum_{i=1}^{n} M_i[(\rho_i^T\rho_i)\mathbf{I}_{3\times3} - \rho_i\rho_i^T]\dot{\omega}_{B_R} \\ &- \mathbf{S}(\omega_{\mathbf{B_R}})\sum_{i=1}^{n} M_i[(\rho_i^T\rho_i)\mathbf{I}_{3\times3} - \rho_i\rho_i^T]\omega_{B_R}\Bigg\}\end{aligned} \tag{56}$$

The inertia matrix of the receiver, excluding fuel, is

$$\underline{\mathbf{I}}_{\mathbf{M}} = \sum_{i=1}^{n} M_i[(\rho_i^T\rho_i)\mathbf{I}_{3\times3} - \rho_i\rho_i^T] \tag{57}$$

Similarly, the inertia matrix of the entire system (receiver and fuel) at a given time can be expressed in the B_R frame:

$$\underline{\mathbf{I}}_{\mathbf{t}} \triangleq \{\underline{\mathbf{I}}_{\mathbf{M}} + \sum_{j=1}^{k} m_j[(\rho_{m_j}^T\rho_{m_j})\mathbf{I}_{3\times3} - \rho_{m_j}\rho_{m_j}^T]\} \tag{58}$$

which is always nonsingular as $\underline{\mathbf{I}}_{\mathbf{M}}$ is a mass property and $\rho_{m_j}^T\rho_{m_j}$ as well as $\rho_{m_j}\rho_{m_j}^T$ are positive definite terms.

The other three lines of Eq. (51) can be rewritten as follows by using the identity in Eq. (A1).

Second line:

$$\begin{aligned}\sum_{j=1}^{k}\{&[\underline{\hat{B}}_R]^T\rho_{m_j} \times \dot{m}_j(\underline{U} + \underline{W}) + [\underline{\hat{B}}_R]^T\rho_{m_j} \times \dot{m}_j[\underline{\hat{B}}_R]^T\dot{\rho}_{m_j} \\ &+ \dot{m}_j[\underline{\hat{B}}_R]^T[(\rho_{m_j}^T\rho_{m_j})\mathbf{I}_{3\times3} - (\rho_{m_j}\rho_{m_j}^T)]\omega_{B_R}\}\end{aligned} \tag{59}$$

Third line:

$$\begin{aligned}\sum_{j=1}^{k}\{&[\underline{\hat{B}}_R]^T\rho_{m_j} \times m_j(\dot{\underline{U}} + \dot{\underline{W}}) + [\underline{\hat{B}}_R]^T\rho_{m_j} \times m_j[\underline{\hat{B}}_R]^T\ddot{\rho}_{m_j} \\ &+ m_j[\underline{\hat{B}}_R]^T[(2\rho_{m_j}^T\dot{\rho}_{m_j})\mathbf{I}_{3\times3} - (2\rho_{m_j}\dot{\rho}_{m_j}^T)]\omega_{B_R} \\ &+ m_j[\underline{\hat{B}}_R]^T[(\rho_{m_j}^T\rho_{m_j})\mathbf{I}_{3\times3} - (\rho_{m_j}\rho_{m_j}^T)]\dot{\omega}_{B_R} \\ &+ m_j(\omega_{B_R}^T\rho_{m_j})[\underline{\hat{B}}_R]^T\rho_{m_j} \times [\underline{\hat{B}}_R]^T\omega_{B_R}\}\end{aligned} \tag{60}$$

Fourth line:

$$-[\underline{\hat{B}}_R]^T\rho_R \times \dot{m}([\hat{I}]^T\dot{r}_{B_T} + [\underline{\hat{B}}_T]^TV_{\dot{m}} - [\underline{\hat{B}}_T]^T\mathbf{S}(\omega_{\mathbf{B_T}})\rho_C) \tag{61}$$

The matrix forms of $\underline{U}$, $\dot{\underline{U}}$, $\underline{W}$, and $\dot{\underline{W}}$ in Eq. (51) can be substituted from Eqs. (34) and (39–41), respectively. Also, ω_{B_R} and $\dot{\omega}_{B_R}$ can be substituted from Eqs. (31) and (32), respectively. Once the vectrices are written in terms of a common vectrix, the common vectrix is eliminated and the result is rearranged. Equation (51) then yields the matrix form of the equations of rotational motion.

$$\begin{aligned}\dot{\omega}_{B_R B_T} = &\underline{\mathbf{I}}_{\mathbf{t}}^{-1}M_{B_R} + \underline{\mathbf{I}}_{\mathbf{t}}^{-1}\mathbf{S}(\omega_{\mathbf{B_R B_T}} + \mathbf{R}_{\mathbf{B_R B_T}}\omega_{\mathbf{B_T}})\underline{\mathbf{I}}_{\mathbf{M}} \\ &\times (\omega_{B_R B_T} + \mathbf{R}_{\mathbf{B_R B_T}}\omega_{B_T}) + \underline{\mathbf{I}}_{\mathbf{t}}^{-1}\sum_{j=1}^{k}\mathbf{S}(\rho_{\mathbf{m_j}}) \\ &\times [m_j(\omega_{B_R B_T}^T + \omega_{B_T}^T\mathbf{R}_{\mathbf{B_R B_T}}^{\mathbf{T}})\rho_{m_j}(\omega_{B_R B_T} + \mathbf{R}_{\mathbf{B_R B_T}}\omega_{B_T}) \\ &+ m_j\ddot{\rho}_{m_j} + \dot{m}_j\dot{\rho}_{m_j}] + \underline{\mathbf{I}}_{\mathbf{t}}^{-1}\left[\sum_{j=1}^{k}\mathbf{S}(\rho_{\mathbf{m_j}})m_j\right] \\ &\times \{-[\mathbf{S}(\omega_{\mathbf{B_R B_T}}) + \mathbf{S}(\mathbf{R}_{\mathbf{B_R B_T}}\omega_{\mathbf{B_T}})](\mathbf{R}_{\mathbf{B_R W_R}}U + W) \\ &+ \mathcal{E}_{\mathbf{R}}\dot{\mathcal{X}}_R + \dot{W}\} + \underline{\mathbf{I}}_{\mathbf{t}}^{-1}\left[\sum_{j=1}^{k}\mathbf{S}(\rho_{\mathbf{m_j}})\dot{m}_j\right](\mathbf{R}_{\mathbf{B_R w_R}}U + W) \\ &- 2\underline{\mathbf{I}}_{\mathbf{t}}^{-1}\sum_{j=1}^{k} m_j[(\rho_{m_j}^T\dot{\rho}_{m_j})\mathbf{I}_{3\times3} - \dot{\rho}_{m_j}\rho_{m_j}^T](\omega_{B_R B_T} + \mathbf{R}_{\mathbf{B_R B_T}}\omega_{B_T}) \\ &- \underline{\mathbf{I}}_{\mathbf{t}}^{-1}\sum_{j=1}^{k}\dot{m}_j[(\rho_{m_j}^T\rho_{m_j})\mathbf{I}_{3\times3} - \rho_{m_j}\rho_{m_j}^T](\omega_{B_R B_T} + \mathbf{R}_{\mathbf{B_R B_T}}\omega_{B_T}) \\ &- \mathbf{S}(\omega_{\mathbf{B_R B_T}})\mathbf{R}_{\mathbf{B_R B_T}}\omega_{B_T} - \mathbf{R}_{\mathbf{B_R B_T}}\dot{\omega}_{B_T} \\ &- \underline{\mathbf{I}}_{\mathbf{t}}^{-1}\dot{m}\mathbf{S}(\rho_R)(\mathbf{R}_{\mathbf{B_R B_T}}\mathbf{R}_{\mathbf{B_T I}}\dot{r}_{B_T} + \mathbf{R}_{\mathbf{B_R B_T}}V_{\dot{m}} \\ &- \mathbf{R}_{\mathbf{B_R B_T}}\mathbf{S}(\omega_{\mathbf{B_T}})\rho_C)\end{aligned} \tag{62}$$

In this equation, all the variables are with respect to the receiver frame or the tanker frame with the exception of $\dot{r}_{B_T}$. As presented previously, the equations of rotational dynamics seem quite

complicated. However, it is very suitable for aerial refueling applications. The angular velocity and the orientation as well as the translational velocity and position of the receiver are defined with respect to the B_T frame. The inertia and mass properties of the receiver before aerial refueling can be directly used in the equation. The effect of refueling on rotational dynamics is represented by the concentrated fuel mass and its c.m. location in each fuel tank. In the case of multiple fuel tanks, the effect of fuel flow into each tank can be taken into account separately. Because the equation is written with respect to a point fixed geometrically in the body of the receiver, a change of the c.m. during refueling is already incorporated in the equation. Another advantage of writing the equation with respect to a frame fixed in the body is seen when the aerodynamic variables such as airspeed, angle of attack, side-slip angle, and aerodynamic stability derivatives are needed. Because these variables and derivatives are determined by the geometric shape of the aircraft, and not its mass properties, standard definitions can be directly used without any modification or reinterpretation.

V. Modeling Wind Effects

The wind effect terms constituting the elements W and $\dot{W}$ in the receiver's equations of motion derived earlier are considered to be based on uniform wind distribution acting at the receiver's c.m., expressed in its body frame. However, the vortex-induced wind field acting on the receiver aircraft is nonuniform in nature. To be able to use the aircraft equations of motion without modification, the nonuniform induced wind components and gradients need to be approximated by uniform wind and gradients. For details of the vortex model and averaging technique applied, see the paper by Dogan et al. [20]. Bound vortices were not considered in this reference whereas they are considered in the present work, but the overall approach of the reference is followed herein.

VI. Application

This section shows how the physical parameters of the receiver aircraft and its fuel tanks are incorporated as mathematical quantities that are included in the derivation of the equations of motion. It also presents results of the simulation that uses the equations of motion developed herein as the model of the receiver aircraft dynamics during aerial refueling. The simulation also includes the full 6-degree-of-freedom nonlinear dynamics of the tanker aircraft. The position and orientation of the receiver relative to the tanker are controlled by a gain-scheduling linear controller while the tanker flies in a racetrack maneuver. The simulation contains the innovative control effectors (ICE) unmanned aircraft as the receiver being refueled from a KC-135 tanker aircraft. For details of the tanker or receiver being simulated or the controller being employed, see [21,22]. Further, Appendix B presents both aircraft data used in the simulation.

A. Fuel Tank Configuration

First, the overall fuel flow rate $\dot{m}$ from the tanker to the receiver is considered to be specified as an external input. The amount of the total fuel that is sent to each individual fuel tank is also specified. For example, Fig. 3 shows the sketch of the ICE aircraft with four fuel tanks. Typically, refueling begins with the forward tanks with a fuel flow distribution of $\dot{m}_1 = \dot{m}_2 = 0.5\dot{m}$ where the combined fuel capacity of tanks 1 and 2 is 35% of the total aircraft fuel. After tanks 1 and 2 are full, the aft tanks are refueled with a similar distribution ($\dot{m}_3 = \dot{m}_4 = 0.5\dot{m}$) where the combined fuel capacity of tanks 3 and 4 is 65% of the total aircraft fuel. The actual mass contained in the jth fuel tank at any instant of time can be computed by integrating $\dot{m}_j$ over time. If there is any residual fuel in the tank before the start of refueling, that can be considered as part of the receiver aircraft. Therefore, without any loss of generality, it is assumed that $m_j(0) = 0$.

The next variable to be determined is $\underline{\rho}_{m_j}$ which is the position vector of the fuel mass concentrated at the jth point, expressed in the B_R frame. Recall the assumption that fuel in each fuel tank is concentrated at its c.m. In general, the initial location $\underline{\rho}_{m_j}(0)$ is considered to be the midpoint of the base of the jth fuel tank or the surface of the remaining fuel. As fuel flows into the fuel tank, the vector $\underline{\rho}_{m_j}(t)$ always points at the c.m. of the fuel under the assumptions that the fuel tanks are rectangular and the fuel stays level within each tank. The position vectors along with their time derivatives for all the fuel tanks are used in the receiver's equations of motion.

B. Simulation Results

Simulation results will now be shown for several cases. The nominal altitude of the tanker is 7010 m with a speed of 190 m/s in a racetrack maneuver. This is only the nominal flight condition; small deviations from the nominal condition occur as the tanker transitions between the legs of the racetrack maneuver. While the tanker flies in the racetrack, the receiver aircraft needs to maintain a contact position of (−25.33, 0, 6.46) m relative to the body frame of the tanker. Maintaining the contact position enables the tanker's refueling boom to deliver 0.04416 m^3 of JP-4 fuel per second (700 gal/min) at the speed of 5.45 m/s. It is assumed that the refueling boom is inclined 30 deg downward from the negative x axis

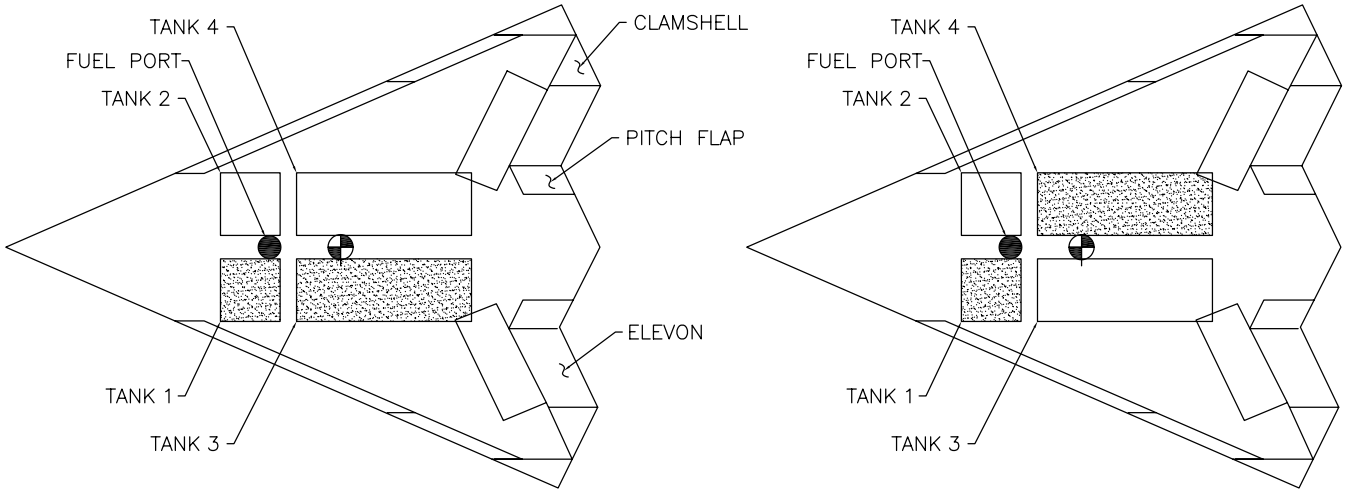

a) b)

Fig. 3 Receiver-fuel tank failure cases: a) Right-hand tanks do not fill and b) right-hand forward and left-hand aft tanks do not fill.

of the tanker's body frame during the fuel transfer. Results are shown with the tanker in 1) straight and level flight and 2) a constant-altitude, constant-speed turn.

Figures 4–7 depict the results of the simulations when executed for a straight and level flight condition for three different cases, shown in the figure legends. Case 1 is a normal refuel scenario. Both forward tanks refuel first, but at half of the maximum flow rate, until each is half full. Next, both aft tanks refuel, again at half of the maximum flow rate, until each is half full. Case 2 is a refuel failure scenario where neither of the right-hand fuel tanks (labeled tank 2 and tank 4 in Fig. 3) receive fuel, but the left-hand forward tank is fully fueled first, followed by the left-hand aft; this failure scenario is depicted in Fig. 3a. Case 3, depicted in Fig. 3b, is a refuel failure scenario where the right-hand forward and left-hand aft tanks do not fill, but the other tanks fully fuel, with the forward tank refueling first. To allow for better comparisons between the case, the fuel tanks in case 1 (normal) only fill to half capacity so that the transition from refueling the forward tanks to the aft tanks occurs at the same time in all three cases. In addition, the postrefuel total aircraft weight for the normal case matches that for the failure cases. In each case, refueling starts 25 s after the start of the simulation.

To be able to maintain the nominal refueling contact position, the deviation from the refueling position as well as the deviation in relative orientation should be minimal. To analyze the performance of the aircraft in terms of these important requirements, the receiver's position and orientation with respect to the tanker in the time domain are presented in Figs. 4 and 5, respectively.

Figure 4 shows spikes in position deviations whenever fuel flow starts or ends in each fuel tank. In Fig. 4, the first such spike at 25 s is the same for both cases 2 and 3 due to the fact that both cases begin by refueling the left-hand forward tank, but case 3 has the largest spike around 70 s as the result of the cessation of tank 1 refueling and the commencement of (right-hand aft) tank 4 refueling. Similarly, the opposite-direction y position spikes at about 140 s are the result of refuel completion and the reorientation of the aircraft into an appropriate trim condition after being refueled in opposite-side aft tanks. Although cases 2 and 3 have, as expected, the same y deviations while tank 1 is filled, their y deviations are in opposite directions due to the fact that opposite-side aft tanks are being filled in these cases (tank 3 in case 2 and tank 4 in case 3). The x deviation is between -0.2 and 0.2 m in all three cases and the z deviation is between -0.1 and 0.15 m. The deviations are smallest for case 1, which results in zero y deviation as expected based on the fuel tank symmetry. This behavior is mathematically represented by the third term of Eq. (48), which illustrates the contribution of the individual fuel tank masses and their derivatives, along with the fuel c.m. locations and their derivatives, to the receiver's translational dynamics.

Figure 5 illustrates the deviation of the receiver orientation from the tanker orientation. The pitch angle variation is approximately the same (below 1.5 deg) for all cases while case 3 causes a greater range of deviation of both yaw and bank angles. As with the y deviation of Fig. 4, the portion of the case 3 yaw deviation which is opposite of the case 2 yaw deviation is due to the asymmetric tank refueling. The opposite-direction tendencies of the yaw and bank angles immediately follow the case 3 transition from the forward to the diagonal aft fuel tank when compared to the same-side forward to aft tank transition of case 2. These moments are largely due to the contribution of the second, third, fourth, fifth, sixth, and eighth terms of Eq. (62), which express the relationship between the derivatives of the individual fuel tank masses and center-of-gravity locations to the receiver's rotational dynamics. After completion of the refueling, the yaw trim angle is different for cases 2 and 3. Case 2 results in a slightly positive yaw trim angle while case 3 results in a very slightly negative yaw trim angle. There is also a, albeit very small, nonzero steady-state bank angle in cases 2 and 3. This demonstrates the effect of the asymmetric mass distribution on the steady-state trim condition.

Figure 6 illustrates the values of the elevon, pitch flap, and clamshell deflections for the three level flight cases. In each case, small deflections (compared to the saturation deflections) are required to maintain the refuel contact position throughout the simulation. Both the elevon and clamshell deflections can be compared with the roll and yaw angle histories in Fig. 5 to show how these effectors react to the refueling in the failure cases and how their steady-state positions correspond to the receiver's steady-state Euler angles. When the refueling of case 3 transitions from the forward to the diagonal aft tank, both the elevon and clamshell react immediately to compensate for the opposite-side tank refueling. The magnitude of the elevon and pitch flap deflections change steadily throughout the refueling to account for the steadily growing fuel tank masses. This is caused by the contribution of the gravitational moment caused by the fuel masses to the total moment of the external forces about the origin of the B_R frame. Figure 7 illustrates the level of throttle in the three cases, which prove to be very similar. As expected, the throttle tends to grow as the refueling occurs (beginning at 25 s) to keep the receiver at the commanded velocity while experiencing mass increase, and the steady-state throttle value is somewhat higher than initially due to the higher postrefuel aircraft weight.

Figures 8–11 depict the results of the simulation when executed for a U-turn maneuver which involves the tanker beginning to turn 25 s into the simulation with a specified yaw rate until the yaw angle change reaches 180 deg. The commanded yaw rate for the tanker in this maneuver is generated from a 1.7 deg/s step response of a fourth order linear filter with time constants of 10, 10, 10, and 1 s. In these figures, case 1 involves the turn maneuver only with no refueling, included as a reference to determine how much of the receiver's response is due solely to the refueling. Case 2 is the same

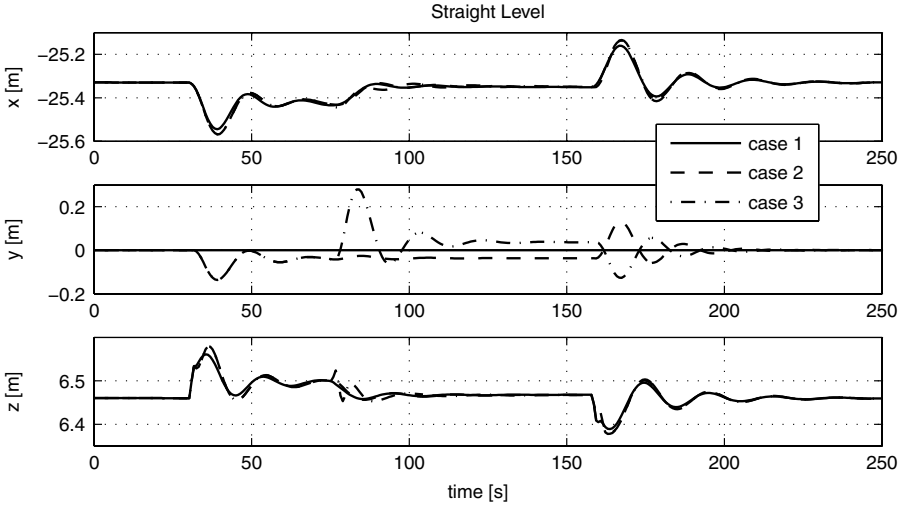

Fig. 4 Time history of the deviation of the receiver position from the refueling position in straight level flight.

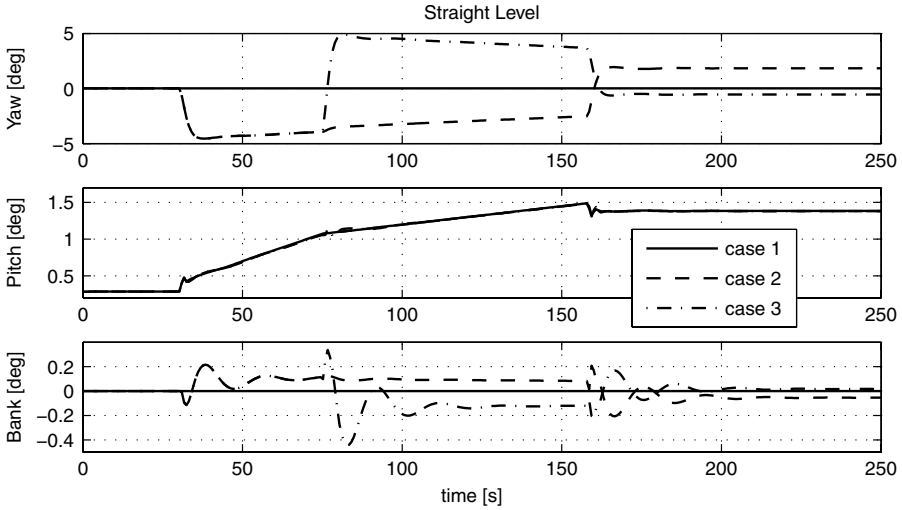

Fig. 5 Time history of the receiver relative orientation deviation in straight level flight.

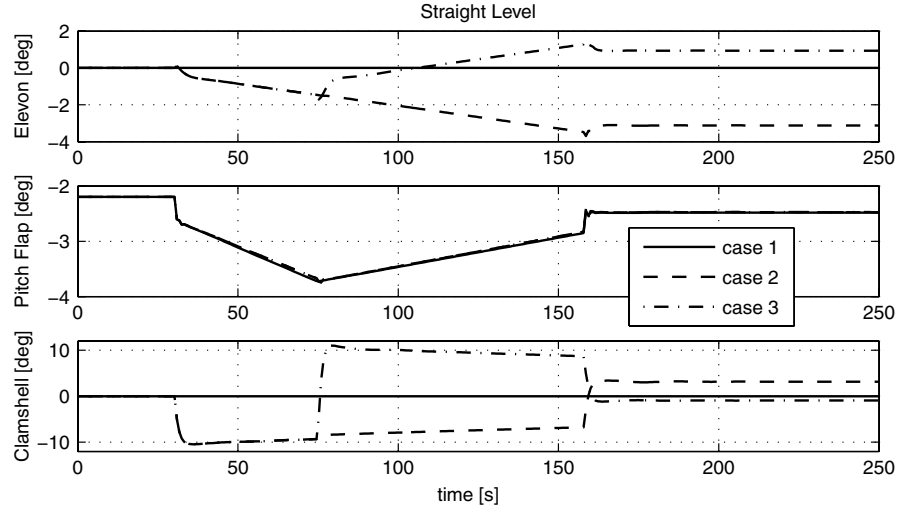

Fig. 6 Time history of receiver control surface deflections in straight level flight.

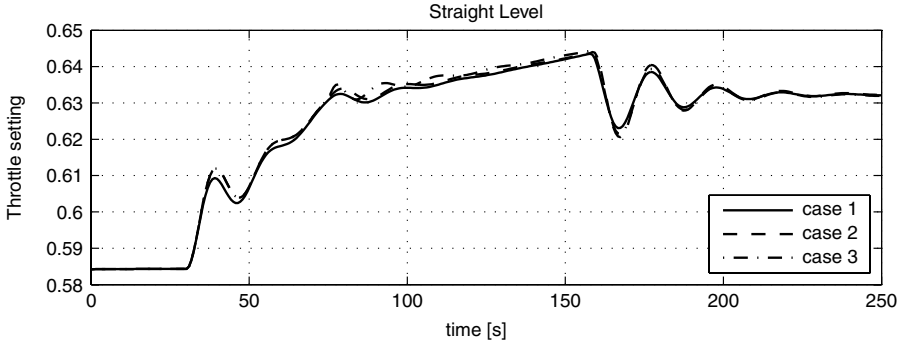

Fig. 7 Time history of receiver throttle setting in straight level flight.

normal refuel scenario introduced in the straight level flight case, with refueling beginning with the forward tanks at 25 s and continuing with the aft tanks after the forward tanks are filled to commanded capacity. Case 3 is the refuel failure scenario where the right-hand forward and the left-hand aft tanks do not fill, which is depicted in Fig. 3b. Once again, the fuel tanks in the normal case are commanded to fill only to half of their capacities so that the transition from refueling the forward tanks to the aft tanks occurs at the same time in cases 2 and 3 while ensuring that the postrefuel total aircraft weight for the normal case matches that for the failure case.

As in the straight level flight case, the deviation from the refueling position as well as the deviation in relative orientation should be minimal. To analyze the performance of the aircraft in terms of this requirement, the receiver's position and orientation with respect to the tanker in the time domain are presented in Figs. 8 and 9, respectively. When compared with deviations in the straight level cases, case 1 for the U-turn maneuver shows that most of the deviations from the commanded refueling position are due to the maneuver itself. However, Figs. 8 and 9 show additional deviations due to the symmetric and asymmetric fuel transfer. The effects of the

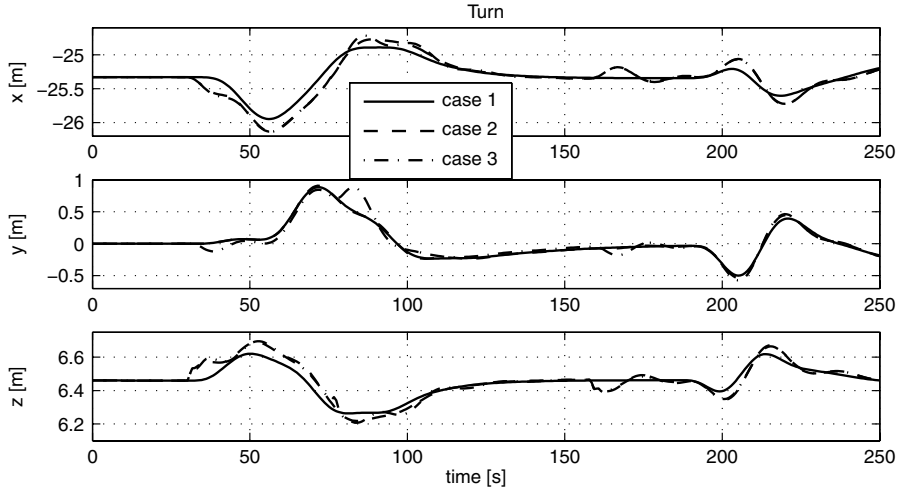

Fig. 8 Time history of the deviation of the receiver position from the refueling position during turn.

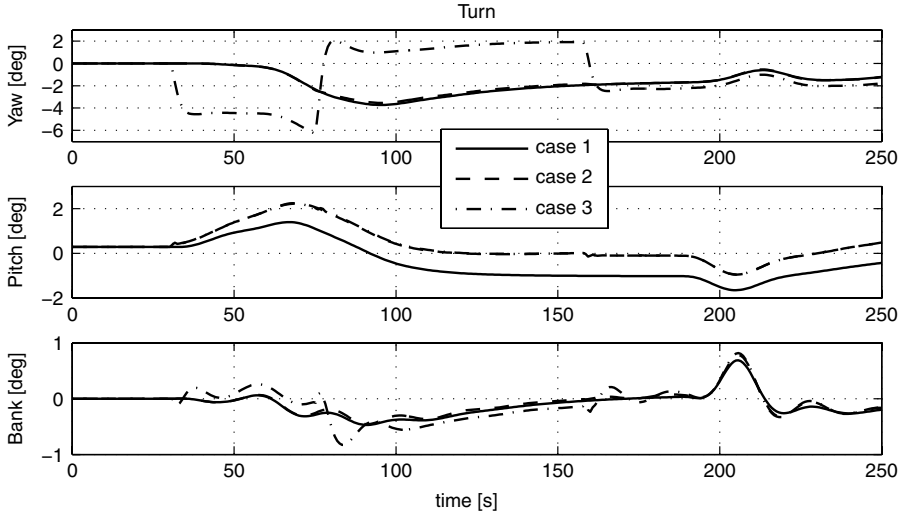

Fig. 9 Time history of the receiver relative orientation deviation during turn.

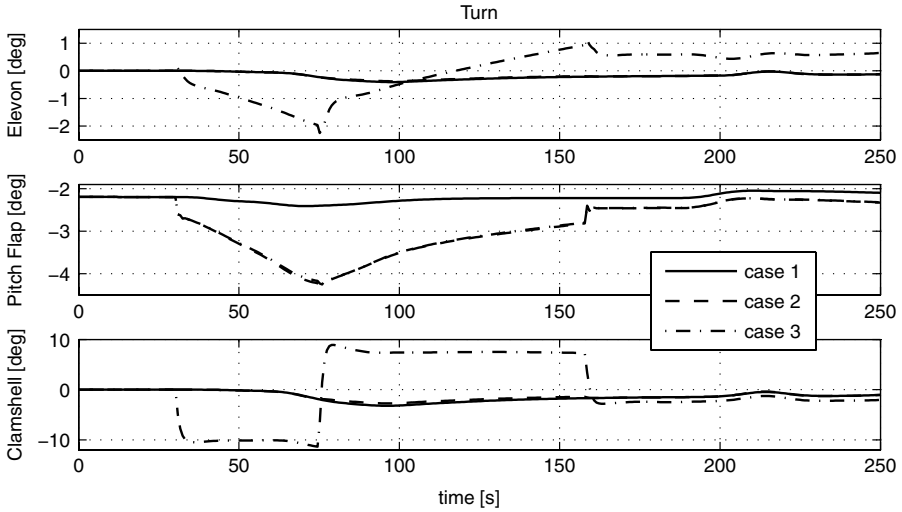

Fig. 10 Time history of receiver control surface deflections during turn.

refueling are somewhat more pronounced in the Euler angle plot of Fig. 9, where both refueling cases, especially the failure of case 3 about the yaw axis, create orientation deviations significantly in excess of the orientation deviations due only to the turn. It is also apparent in this plot that, when compared to the no-refueling case 1, the steady-state pitch angle of cases 2 and 3 is approximately 1 deg higher to account for the increased aircraft weight at the end of the refueling.

Figure 10 illustrates the values of the elevon, pitch flap, and clamshell deflections for the three turning flight cases. The

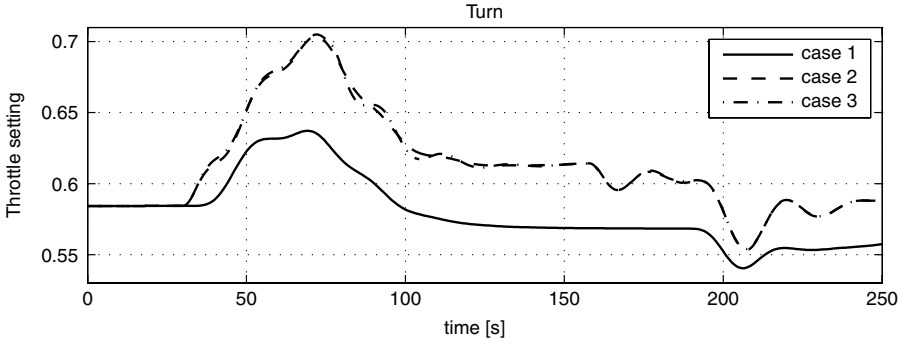

Fig. 11 Time history of receiver throttle setting during turn.

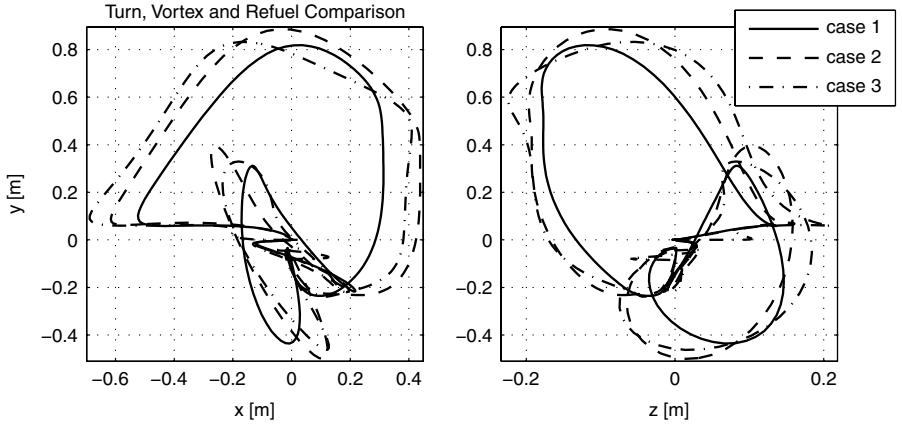

Fig. 12 Deviation of the receiver position from the refueling position during turn for observation of vortex and refueling effects.

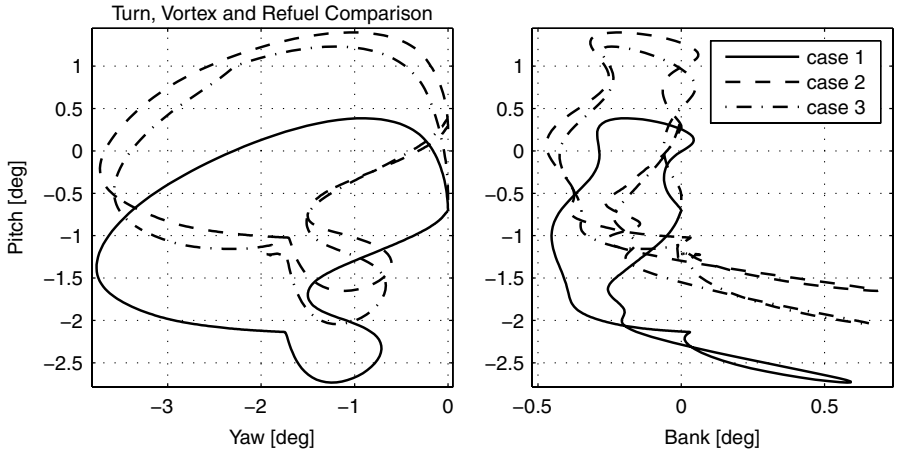

Fig. 13 Receiver deviation in relative orientation during turn for observation of vortex and refueling effects.

magnitudes and trends are very similar to those found in the level flight cases. The differences between the effector deflections required for turning with and without refueling are also illustrated here, with the steady-state trim deflections somewhat different both with and without fuel, and with and without asymmetric mass distribution. Figure 11 illustrates the level of throttle in the three cases, with cases 2 and 3 having almost identical throttle requirements. The throttle setting is higher in cases 2 and 3 than in case 1 during the turn as well as during the steady state after the turn and refueling are both completed. This is due to the mass transfer during the refueling and due to the higher postrefuel aircraft weight in steady state.

Finally, Figs. 12 and 13 are presented as a means of comparing the effect of the vortex on the receiver position and orientation deviations to the effect of the refueling in the turn scenario. In these figures, case 1 is a simulation involving neither the vortex nor the refueling and is included as a reference for the other two cases. In case 2, the vortex is included without any refueling, while case 3 includes refueling at 25 s as before, but with no vortex. By comparing the effects of the vortex and refueling in isolation, it is apparent that the relative contribution to the overall deviations in position is similar. From this result, it seems reasonable to conclude that the effect of the refueling (and associated mass properties changes) is as significant to the performance of the receiver as the effect of the vortex-induced wind field.

VII. Conclusions

A set of equations of motion of an aircraft is derived to account for time-varying inertia properties due to fuel transfer and exposure to wind induced by the wake vortex of a lead aircraft.

The receiver is modeled so as to allow for mass center shift of the system during fuel transfer. Modeling of the refueling system allows for time-varying fuel quantity and center of mass for each fuel tank individually, as well as the specification of fuel tank location, shape, and size. Further, the speed and direction of fuel flow into the receiver, as well as the location of the receptacle in the receiver, are accounted for.

The dynamic effect of wind exposure appears explicitly in the derived equations of motion. The equations are expressed in terms of the position and orientation of the receiver relative to the tanker, rather than relative to the inertial frame. The equations are thus particularly suited to the aerial refueling problem because aerial refueling requires control of the receiver relative to the tanker.

The equations are presented in matrix form for ease of simulation. This study shows that, during both straight level flight and a U-turn maneuver, the capability to maintain the refuel contact position is most degraded during a diagonal, asymmetric refueling failure scenario. There are significant dynamic repercussions associated with refueling failures resulting in fuel entering a tank on only one side of the aircraft centerline. The simulation additionally reveals that the dynamic effect of the tanker trailing vortex is as significant as the time-varying mass dynamic effect on the receiver aircraft. The generic nature of the developed equations permits the simulation of any type of aircraft at any flight condition with mass transfer or mass variation of any sort. The main limitations of the equations derived are that the fuel tanks are modeled point masses and fuel flow is taken to be steady.

Appendix A: Matrix and Vector Properties

This Appendix presents easy referencing for some of the matrix and vector properties used in the derivation of the equations of motion.

Fact 1: Quadruple product of vectors

$$\underline{a} \times [\underline{b} \times (\underline{c} \times \underline{d})] = (\underline{b} \cdot \underline{d})\underline{a} \times \underline{c} - (\underline{b} \cdot \underline{c})\underline{a} \times \underline{d}, \quad \forall\ \underline{a}, \underline{b}, \underline{c}, \underline{d} \tag{A1}$$

Fact 2: Vector product of vectors through their representations

$$\underline{a} \times \underline{b} = [\hat{\underline{1}}]^T a \times [\hat{\underline{1}}]^T b = -[\hat{\underline{1}}]^T \mathbf{S}(a) b \tag{A2}$$

where a and b are representations of $\underline{a}$ and $\underline{b}$, respectively, in the frame having vectrix $[\hat{\underline{1}}]$, and $\mathbf{S}(a)$ is the skew-symmetric matrix

$$\mathbf{S}(a) = \begin{bmatrix} 0 & a_3 & -a_2 \\ -a_3 & 0 & a_1 \\ a_2 & -a_1 & 0 \end{bmatrix} \tag{A3}$$

for vector $\underline{a}$ with representation $[\,a_1 \quad a_2 \quad a_3\,]^T$ in the frame having vectrix $[\hat{\underline{1}}]$.

Fact 3: Order of vectors in vector product

$$\mathbf{S}(a) b = -\mathbf{S}(b) a \tag{A4}$$

Fact 4:

$$(a^T b)\mathbf{S}(a) = -\mathbf{S}(b) a a^T \quad \forall\ a, b \tag{A5}$$

Fact 5:

$$\mathbf{S}(\mathbf{R}_{21} a) = \mathbf{R}_{21} \mathbf{S}(a) \mathbf{R}_{21}^{\mathbf{T}} \tag{A6}$$

Appendix B: Numerical Data

I. Simulation Parameters

Formation flight velocity: 190 m/s
Formation flight altitude: 7010 m

II. Receiver Aircraft Parameters

M: 1.1281×10^4 kg
ρ_r in the B_R frame: $[\,1.5738 \quad 0 \quad -0.7239\,]^T$ m
Forward tank capacity: 2148 kg
Aft tank capacity: 3898 kg
Wing area S: 75.12 m^2
Wing mean chord $\bar{c}$: 8.763 m
Wing span b: 11.43 m
Fuselage diameter D_f: 1.4478 m
Fuselage length L_f: 13.158 m
x distance between the c.g. of the aircraft and the aerodynamic center of the wing: 0.0101 m
z distance between the c.g. of the aircraft and the aerodynamic center of the wing: 0 m
Dihedral angle ζ: 0 deg
Sweepback angle at quarter-chord λ: 0.2487 rad
Inertia matrix, kg $\cdot$ m^2: $I_{xx} = 3.186 \times 10^4$, $I_{yy} = 8.757 \times 10^4$, $I_{zz} = 1.223 \times 10^5$, $I_{xz} = -546.394$
Aerodynamic coefficients [22]: $C_{D0} = 0.023$, $C_{D\alpha} = 0$, $C_{D\alpha^2} = 0.7$, $C_{D\delta e} = 0$, $C_{D\delta e^2} = 0.25$, $C_{S0} = 0$, $C_{S\beta} = -0.031$, $C_{S\delta_r} = 0$, $C_{L0} = 0.062$, $C_{L\alpha} = 2.09$, $C_{L\alpha 2} = 0$, $C_{Lq} = 1.53$, $C_{L\delta_e} = 0.594$, $C_{\mathcal{L}0} = 0$, $C_{\mathcal{L}\delta_a} = -0.13$, $C_{\mathcal{L}\delta_r} = -0.004$, $C_{\mathcal{L}\beta} = -0.022$, $C_{\mathcal{L}p} = -0.163$, $C_{\mathcal{L}r} = 0.012$, $C_{\mathcal{M}0} = -0.003$, $C_{\mathcal{M}q} = -0.4$, $C_{\mathcal{M}\alpha} = -0.024$, $C_{\mathcal{M}\delta_e} = -0.169$, $C_{\mathcal{N}0} = 0$, $C_{\mathcal{N}\delta_a} = -0.017$, $C_{\mathcal{N}\delta_r} = -0.018$, $C_{\mathcal{N}\beta} = -0.021$, $C_{\mathcal{N}p} = -0.023$, and $C_{\mathcal{N}r} = -0.009$.

III. Tanker Aircraft Parameters

$V_{\dot{m}}$ in the B_T frame: $[\,-4.7175 \quad 0 \quad 2.7237\,]^T$ m/s
$\dot{m}$: 35.46 kg/s
M: 8.838×10^5 kg
Wing area S: 226.03 m^2
Wing mean chord $\bar{c}$: 6.144 m
Wing span b: 39.877 m
Fuselage diameter D_f: 3.657 m
Fuselage length L_f: 39.267 m
x distance between the c.g. of the aircraft and the aerodynamic center of the wing: -0.823 m
z distance between the c.g. of the aircraft and the aerodynamic center of the wing: 0.304 m
Dihedral angle ζ: 7 deg
Inertia matrix, kg $\cdot$ m^2: $I_{xx} = 3.592 \times 10^6$, $I_{yy} = 3.430 \times 10^6$, $I_{zz} = 7.090 \times 10^6$, $I_{xz} = 5.152 \times 10^4$
Aerodynamic coefficients [22]: $C_{D0} = 0.028$, $C_{D\alpha} = 0$, $C_{D\alpha^2} = 0.2642$, $C_{D\delta e} = 0$, $C_{S0} = 0$, $C_{S\beta} = -0.812$, $C_{S\delta_r} = 0.184$, $C_{L0} = 0.1$, $C_{L\alpha} = 4.8$, $C_{L\alpha 2} = 0$, $C_{Lq} = 5.65$, $C_{L\delta_e} = 0.19$, $C_{\mathcal{L}0} = 0$, $C_{\mathcal{L}\delta_a} = -0.05$, $C_{\mathcal{L}\delta_r} = 0.019$, $C_{\mathcal{L}\beta} = -0.177$, $C_{\mathcal{L}p} = -0.312$, $C_{\mathcal{L}r} = 0.153$, $C_{\mathcal{L}\delta_e} = 0$, $C_{\mathcal{M}0} = 0$, $C_{\mathcal{M}q} - 4.5$, $C_{\mathcal{M}\alpha} = -0.65$, $C_{\mathcal{M}\delta_e} = -0.57$, $C_{\mathcal{N}0} = 0$, $C_{\mathcal{N}\delta_a} = 0.008$, $C_{\mathcal{N}\delta_r} = -0.076$, $C_{\mathcal{N}\beta} = 0.129$, $C_{\mathcal{N}p} = -0.011$, and $C_{\mathcal{N}r} = -0.165$.

References

[1] Pachter, M., Houpis, C., and Trosen, D., "Design of an Air-To-Air Automatic Refueling Flight Control System Using Quantitative Feedback Theory," *International Journal of Robust and Nonlinear Control*, Vol. 7, No. 6, 1997, pp. 561–580. doi:10.1002/(SICI)1099-1239(199706)7:6<561::AID-RNC291>3.0.CO;2-V

[2] Bloy, A., West, M., Lea, K., and Jouma, M., "Lateral Aerodynamics Interference Between Tanker and Receiver in Air-To-Air Refueling," *Journal of Aircraft*, Vol. 30, No. 5, 1993, pp. 705–710. doi:10.2514/3.46401

[3] Bloy, A., and West, M., "Interference Between Tanker Wing Wake with Roll-Up and Receiver Aircraft," *Journal of Aircraft*, Vol. 31, No. 5, 1994, pp. 1214–1216. doi:10.2514/3.46633

[4] Bloy, A., and Lea, K., "Directional Stability of a Large Receiver Aircraft in Air-to-Air Refueling," *Journal of Aircraft*, Vol. 32, No. 2, 1995, pp. 453–455. doi:10.2514/3.46741

[5] Singh, S., Chandler, P., Schumacher, C., Banda, S., and Pachter, M., "Nonlinear Adaptive Close Formation Control of Unmanned Aerial

Vehicles," *Dynamics and Control*, Vol. 10, No. 2, 2000, pp. 179–194. doi:10.1023/A:1008348025564

[6] Tsuda, Y., and Shinichi, N., "New Attitude Motion Following Control Algorithm for Capturing Tumbling Object in Space," *Acta Astronautica*, Vol. 53, No. 11, 2003, pp. 847–861. doi:10.1016/S0094-5765(02)00213-8

[7] Isao, K., Mokuno, M., Toru, K., and Suziki, T., "Result of Automous Rendezvous Docking Experiment of Engineering Test Satellite-VII," *Journal of Spacecraft and Rockets*, Vol. 38, No. 1, Jan.–Feb. 2001, pp. 105–111. doi:10.2514/2.3661

[8] Singla, P., Subbarao, K., and Junkins, J. L., "Adaptive Output Feedback Control for Spacecraft Rendezvous and Docking Under Measurement Uncertainty," *Journal of Guidance, Control, and Dynamics*, Vol. 29, No. 4, 2006, pp. 892–902. doi:10.2514/1.17498

[9] Hess, R., "A Simplified Technique for Modeling Piloted Rotorcraft Operations Near Ships," AIAA Paper 2005-6030, 2005.

[10] Rosser, J. B., Newton, R. R., and Gross, G. L., *Mathematical Theory of Rocket Flight*, McGraw–Hill, New York, 1947, pp. 1–16.

[11] Jarmolow, K., "Dynamics of a Spinning Rocket with Varying Inertia and Applied Moment," *Journal of Applied Physics*, Vol. 28, No. 3, 1957, pp. 308–313. doi:10.1063/1.1722736

[12] Ellis, J. W., and McArthur, C. W., "Applicability of Euler's Dynamical Equations to Rocket Motion," *ARS Journal*, Vol. 29, No. 11, 1959, pp. 863–864.

[13] Thomson, W. T., *Introduction to Space Dynamics*, Dover Publications, Inc., Mineola, NY, 1986, pp. 220–236.

[14] Eke, F. O., Mao, T. C., and Morris, M. J., "Free Attitude Motions of a Spinning Body with Substantial Mass Loss," *Journal of Applied Mechanics*, Vol. 71, No. 2, 2004, pp. 190–194. doi:10.1115/1.1653738

[15] Bennington, M. A., and Visser, K. D., "Aerial Refueling Implications for Commercial Aviation," *Journal of Aircraft*, Vol. 42, No. 2, 2005, pp. 366–375. doi:10.2514/1.4770

[16] Bloy, A., and Khan, M., "Modeling of the Receiver Aircraft in Air-to-Air Refueling," *Journal of Aircraft*, Vol. 38, No. 2, 2001, pp. 393–396. doi:10.2514/2.2775

[17] Jewell, W., and Stapleford, R., "Mathematical Models Used to Simulate Aircraft Encounters with Wake Vortices," STI TR 1035-4, 1975, pp. 38–57.

[18] Pachter, M., D'Azzo, J., and Proud, A., "Tight Formation Flight Control," *Journal of Guidance, Control, and Dynamics*, Vol. 24, No. 2, 2001, pp. 246–254. doi:10.2514/2.4735

[19] Johnson, W., Teper, G., and Rediess, H., "Study of Control System Effectiveness in Alleviating Vortex Wake Upsets," *Journal of Aircraft*, Vol. 11, No. 3, 1974, pp. 148–154. doi:10.2514/3.60340

[20] Dogan, A., Venkataramanan, S., and Blake, W., "Modeling of Aerodynamic Coupling Between Aircraft in Close Proximity," *Journal of Aircraft*, Vol. 42, No. 4, July–Aug. 2005, pp. 941–955. doi:10.2514/1.7579

[21] Dogan, A., Kim, E., and Blake, W., "Control and Simulation of Relative Motion for Aerial Refueling in Racetrack Maneuvers," *Journal of Guidance, Control, and Dynamics*, Vol. 30, No. 5, 2007, pp. 1551–1557. doi:10.2514/1.29487

[22] Kim, E., "Control and Simulation of Relative Motion for Aerial Refueling in Racetrack Maneuver," M.S. Thesis, The University of Texas at Arlington, Arlington, TX, May 2007.